Available online at www.sciencedirect.com
SCIENCE DIRECT
Cement and Concrete Research 36 (2006) 634 – 649
Cement and Concrete Research

The influence of different drying methods on cement paste microstructures as reflected by gas adsorption: Comparison between freeze-drying (F-drying), D-drying, P-drying and oven-drying methods

A. Korpa *, R. Trettin

Institute of Building and Materials Chemistry, University of Siegen 57068, Germany

Received 28 November 2005; accepted 30 November 2005

Abstract

Drying of cement pastes is required prior to microstructure investigation by means of gas adsorption technique. An ideal drying method, which would give reproducible results that could perfectly remove only the non-bound water and, at the same time, preserve the microstructure, unfortunately does not exist. The different drying methods used affect the microstructures in different ways. However, an effective water removal and, less damaging drying method between the common methods used would be still of outstanding importance for sample preparation. Many drying methods have been investigated in the past for such a purpose, and a good agreement for the best drying method does not exist. The so-called D-drying method is being used in many laboratories as the "best" method for drying cement pastes. The surface areas and pore size distributions results of the current work confirm that D-drying (D-Drying C^{-t}) is a relatively good preservation and effective drying method, and that Freeze-drying gives slightly better results compared to D-drying (C^{-t}) and other methods. However the short time versions of some of these methods indicate the presence of very few "micropores", which are not present with prolonged drying times. The outgas level is also a very important variable affecting the gas adsorption measurements especially in the case of short duration drying conditions, as indicated by the results of this work.

Keywords: Cement paste; Drying; Pore size distribution; Microstructure

1. Introduction

Cement pastes have a characteristic pore structure which depends primarily on the w/c ratio, the extent and conditions of hydration, and, to a lesser extent, on the specific cement used, the presence or absence of admixtures and certain other factors [1]. The pores stem mostly from what were originally water-filled spaces between cement particles, and finer pores, below around 2 nm, are believed to be characteristic internal features of C–S–H gel: the main hydration product of cement paste [1]. The pores form an interconnected network, although at low water/cement ratios the connections may become largely plugged by hydration products. Because of this interconnection, it is often not possible to delineate the boundaries of a given individual "pore" [1]. The high surface area of hydrated PC is primarily due to the porous microstructure of the main hydration product, $CaO–SiO_2–H_2O$ (C–S–H) [2]. To measure the surface area by the gas adsorption technique, the water stored in the pores must be removed. It is thought that two general types of pores are present in C–S–H gel, both of which contain water; capillary pores are larger pores that hold water in saturated conditions but lose their water on exposure to air, and gel pores are nanometer-sized pores (<2 nm). The water that is present in gel pores is more strongly bound than capillary water and can be removed only by drying the paste. Any gel pores which remain filled with water will not be accessed by the adsorbate molecules and will not be included in the surface area measurement [2]. The smallest pores are the most difficult to empty of water, but they also have the highest relative surface area, and the stresses related to surface tension of the receding water menisci generate a collapse of some of the fine pores, which are the most sensitive to these capillary effects [3]. It has often been suggested by other authors that the drying

* Corresponding author.
E-mail address: korpa@chemie.uni-siegen.de (A. Korpa).

0008-8846/$ - see front matter © 2005 Elsevier Ltd. All rights reserved.
doi:10.1016/j.cemconres.2005.11.021

process partially destroys or alters the C–S–H gel structure, causing gas adsorption measurements to measure too low a surface area even after adequate drying (water removal) [2]. Therefore various drying methods have been developed to preserve its structure. The various drying methods generates very different surface area and porosity values, depending on the drying method used, even though the same sorption conditions are applied [2]. A right understanding of the C–S–H nanostructure and its characterizing porosity is of major importance in influencing and improving the bulk properties of the hardened cement, such as compressive strength, freeze–thaw behaviour, permeability and ion migration, which are directly related to the pore structure. Adsorption measurements using various adsorbates (N_2, H_2O, Kr, etc.) on a "free surface" generate values of specific surface areas and porosities, and are performed in order to elucidate the C–S–H structure. In the literature the typical values for specific surface area measured by N_2 (SN_2) varies between 10 and 150 m^2/g of dried paste (a little higher by using solvent exchange method) and around 200 m^2/g by using H_2O as adsorbent (SH_2O) [2]. Interpretation of the generated data are dependent on the conceptual nanostructural model adopted for the C–S–H. Various conceptual models of the C–S–H structure were developed during the past years, urged mainly to explain the differences between specific surface areas measured by different adsorbates, namely H_2O and N_2. During the early 1960s, Powers and Brunauer developed a model (Powers–Brunauer model) which states that C–S–H gel consists of randomly arranged colloidal particles, each containing a few closely bonded structural layers. On drying, these layers collapse and do not permit reentry of water. Also, the dried cement paste contains many "ink-bottle" gel pores which water molecules could enter but that larger N_2 molecules could not, so that H_2O sorption measured the full surface area of cement paste [4], [5]. In the 1970s the Feldman–Sereda model also described the basic structural unit of C–S–H gel as a layer, but instead of forming particles, the layers are distributed randomly so that occasional "interlayer spacings" form throughout the C–S–H gel. According to this model, water vapor can move reversibly in and out of these interlayer spacings, which distorts the surface area measurements made with water, and thus in nitrogen which provides the more accurate measure of surface area [6]. Feldman [7] and Helmuth [8] conclusions on the subject matter were that the drying method did not prevent reentry of water, giving evidence that the collapsed structure resulting after drying could be reopened again at a certain extent to permit the reentry of water molecules. The "water"-isotherm exhibited large primary and secondary hysteresis independent of drying method. It was concluded that C–S–H was a poorly crystalline layered material. From the work of Litwan [9] and Litwan and Myers [10] it was apparent that the value of the nitrogen surface area is path dependent with respect to the water isotherm. The value varies significantly when the drying path shifts from one scanning loop to another prior to "final outgassing". Rewetting from an intermediate humidity prior to outgassing "preserves" the structure to a significant extent. In the early 1980s the Munich model considers the C–S–H gel made up of discrete particles bonded together by van der Waals forces, with a bonding strength strongly affected by moisture content. As with Feldman–Sereda model, this model predicts that water vapor interacts with C–S–H gel structure, making it unsuitable for surface area measurements [11]. In the 1990s the Jennings–Tennis model proposed that the pore space of a given cement microstructure can be divided into two regions with fixed volumes, one that nitrogen can penetrate and one that it cannot. The C–S–H gel is modeled as being made up of particles of a fixed size which can exist in either region [12]. These main conceptual models and other ones suggest a "layered structure" for the C–S–H units, which has implications for surface area measurements [13]. This relates to collapse of the structure which can be followed by the diffusion of helium gas into the C–S–H structure at low relative humidities [14]. The water adsorption isotherm technique has proved successful for materials with pore structures that remain stable on removal or addition of water. Measurements for hydrated Portland cement, which is sensitive to stress, drying and exposure to different humidities, are difficult to interpret. On exposure to water the dried material may also rehydrate [15], invalidating in this way the surface area measurements. Gas adsorption, using nitrogen as adsorbent, is being used successfully for the characterization of various porous systems (adsorbents, catalysts, pigments and other porous materials) and shows many advantages compared to other techniques [16]. Despite the difficulties associated with nitrogen adsorption characterization and its uncertainties, however when some criteria are also met for measurements with cement pastes, its results provide considerable information for the C–S–H gel and cement paste morphology. In this work, the attention is focused on the drying method applied to cement pastes, prepared in the same way, for further investigation by nitrogen gas adsorption. A comparison between typical drying methods, concerning specific surface areas and pore size distributions, is carried out by using the drying method and outgas level as variables affecting the preparation results.

2. Experimental

All the pastes for the reported studies were made of commercial PC type I 42.5 R produced in Germany. The chemical and mineral compositions (Bogue) are shown in Table 1. In order to have the same representative sample for each experiment, the cement powder, immediately after having been received, was sampled by using a sampling apparatus (Probenverteilung). The results of such sampling were checked by scanning the particle size distributions for randomly chosen samples from the total samples, and the comparative results for the efficiency of such sampling is shown in Fig. 1. Sample preparation was similar to the method used by Garci Juenger and Jennings [17]. Pastes were cast with a w/c ratio of 0.45 as a common ratio used by other authors in similar works [17,18] and as a theoretical ratio that cannot prevent the complete hydration of cement powder in normal conditions. Batches were small, namely 14,500 g (10,000 g cement powder + 4500 g distilled water). Mixing of cement powder with water and grounding of hardened cement pastes were carried out in a glove box under an Argon gas atmosphere of analytical grade

Table 1
Chemical analysis of PC type I 42.5 R

Phase composition	Weight percent	Mineral composition (by Bogue equations)
SiO_2	17.67	C_3S=63.82%
Al_2O_3	5.78	C_2S=2.514%
TiO_2	–	C_3A=7.72%
Fe_2O_3	4.49	C_4AF=13.66%
Mn_2O_3	0.72	Blain area=3865 cm^2/g
CaO	62.33	
MgO	1.22	
SO_3	3.02	
K_2O	0.80	
Na_2O	0.14	
Properties		
Loss on ignition (LOI)	2.93	
Insoluble residue	0.47	
Free sulfur content	–	
Chlorine ion (Cl^-) content	0.035	
Iron II oxide	–	
Magnesium II oxide	1.22	

purity in order to prevent possible carbonatisation. Mixing was done by hand for 5 min using a stainless steel spatula. Samples were cast in polystyrene vials and sealed in airtight containers in a water bath at 18 °C for the first 24 h. After 24 h of initial hydration, the containers were filled with limewater, sealed and stored again in a water bath at 18 °C for the curing period of 28 days. After the specified time of hydration, samples were removed from the molds and were ground (under an Ar atmosphere) to particle sizes in the range of 600–1200 μm. Each ground sample was divided into two parts; the smaller parts, containing only particles in the range 600–1200 μm were used for gas adsorption and ^1H NMR analysis. The larger parts, containing the aforementioned particle sizes and also a very small quantity of particles smaller than the specified range (<600 μm), were used for thermogravimetry analysis (water removal after drying and weight change after ignition at 1005 °C). After 28 days, the hydration degree was found to be approximately 0.75 (75%), as calculated by the loss on ignition technique referring to the 24 h oven-dried sample at 105 °C. The schedule of all experimental procedures was planned such that no samples which would have to be stored prior to gas adsorption measurements were generated. This was done in order that the measurements could not be affected by the storing time variable. Ageing effects that manifest themselves as a decrease in nitrogen surface area are well known and documented by others [19].

2.1. The drying methods used in this study

2.1.1. D-drying method

For the D-drying method, the same apparatus as the original one described in the work of Copeland and Hayes was used in this study with the exception that the vacuum pump used could maintain a pressure of 15×10^{-3} Torr instead of 30×10^{-3} Torr [20]. This apparatus consists of a vacuum desiccator connected to the side arm of a trap by a large bore glass tubing. The trap is held at the temperature of a dry ice–alcohol bath (−79 °C), at which temperature the water vapor pressure is about 5×10^{-4} Torr. A layer of corrugated cardboard around the trap extends close to the bottom of the trap. This cardboard is completely covered with rubber tape and serves as an insulating barrier between the trap and the dry ice in the Dewar jar. The trap is connected to a mechanical pump. A small mercury-sealed vacuum stopcock sealed into the side arm is used to break the vacuum when samples are to be removed from the desiccator, which is opened in an "Ar glove box". The vacuum maintained by the pump plays a role on the drying rate, therefore the time required for attaining the weight rate loss of 0.001 g per gram of paste was a little shorter. This method was used to dry samples for 12 h and to dry until a weight loss of 0.001 g per gram of paste and day of drying was reached, named as "D-drying C^{-t}". This rate of weight loss is a value of compromise for accuracy and for speed of drying as argued by the cited authors [20]. The time needed to reach such a rate loss depends on many factors, the most important being the vacuum level maintained by the vacuum pump used, and, of course, of the sample weight being evacuated and the grain sizes. The D-drying method is favored by many cement laboratories as the best standard drying method, and is believed

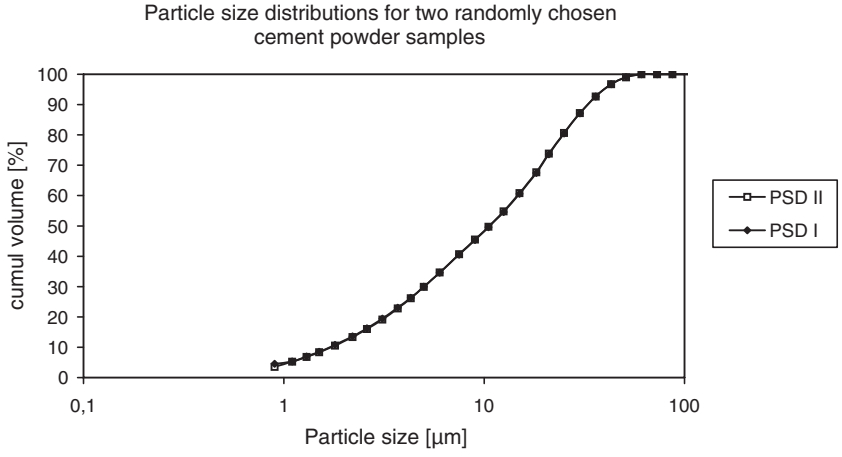

Fig. 1. Sampling efficiency by using a sampling apparatus (Probenverteilung).

to be efficient in removing completely the "non-bound" water and to be the best microstructure preserving drying method compared to other methods [21]. Short drying time versions of the D-drying method are also reported as good preserving methods for drying some cement paste phases prior to investigation [22]. Twelve hours of D-drying (12 h D-drying) is an arbitrarily chosen time for drying in this study, and was chosen in order to compare its efficiency or implications with the other drying methods used. The final vacuum maintained in the system by using the combination of a mechanical vacuum pump and dry ice–alcohol bath (−79 °C) is around 5×10^{-4} Torr. (For a detailed description of "D"- and "P-drying" methods the reader is suggested to consult Ref. [20]).

2.1.2. P-drying method

With the P-drying method, samples are dried to "constant weight" in a sealed system charged with magnesium perchlorate. $Mg[ClO_4]_2 \cdot 2H_2O$ of analytical grade purity was used and the quantity was calculated stoichiometrically based on the initial water quantity used for hydration, the approximate degree of hydration reached after 28 days and on the water quantity needed for the equilibrium reaction $Mg[ClO_4]_2 \cdot 2H_2O + 2H_2O \rightarrow Mg[ClO_4]_2 \cdot 4H_2O$. This is an approach which gives one the possibility to make sure that the minimum quantity of the desiccant required for such an equilibrium is present (accounting also for a tolerance). The partial aqueous vapor pressure for the equilibrium $Mg[ClO_4]_2 \cdot 2H_2O$–$Mg[ClO_4]_2 \cdot 4H_2O$ is reported to be around 8×10^{-3} Torr at RT conditions over the magnesium perchlorate hydrates [23]. Prior to the beginning of the experiment, the desiccator containing the desiccant was separately evacuated (15 min), and then sealed again during the drying time, so that the partial internal pressure was due only to the aqueous vapors. Drying was monitored until the desired weight loss of 0.001 g per gram of paste per day of drying was reached (P-drying C^{-t}), which is considered as constant weight.

2.1.3. Freeze-drying

With the Freeze-drying (F-drying C^{-t}) method samples are submerged in liquid nitrogen and frozen, subsequently the treatment is followed by evacuation. This method was performed using an improvised system consisting of a small desiccator (the same desiccator as that used for P-drying method), which was placed in a circulating, controlled cooling system. The temperature on the sample surface inside the small desiccator was maintained at -10 ± 1 °C. This relatively higher temperature than that used by the common freeze-drying apparatus was chosen to promote a shorter drying time "equilibrium" as in the case of the D-drying method. The same vacuum pump which was used for the D-drying methods (15×10^{-3} Torr) was connected to the desiccator by using a tube having the same diameter as the connecting tube used for the D-drying apparatus. The same vacuum pump was chosen in order not to affect the drying rate artificially by the vacuum level maintained in the system. The same criteria for weight loss (0.001 g water per gram of paste) was taken at the end of the drying time (F-drying C^{-t}). The samples dried by means of F-drying were first frozen by immersing the sample containers in liquid N_2 (−196 °C) for about 5 min and then transferred for drying to the improvised freeze-dryer system. The freeze-drying method is reported as effective with regard to microstructure preservation due to the softening of capillary stress effects generated at solid–water–vapor boundaries during normal drying [24,25].

2.1.4. Oven-drying method

The oven-drying method was performed in a ventilated and temperature programmed oven. Two drying time durations were chosen: oven-drying at 105 ± 1 °C for 3 h and oven-drying at 105 ± 1 °C for 24 h. Oven-drying at 105 °C for 24 h is reported as the most efficient standard method for removing completely the "non-bound" water and also as the most damaging to the microstructure [25,26]. The simple standard method of calculating approximately the hydration degree is based also on this method. The oven-drying method for 3 h at 105 °C was chosen for comparison with the other drying methods used, as an efficient water removal method and also probably as a microstructure preserving one, as suggested by other authors [26]. A lower temperature for oven-drying was not chosen because it was judged that, at such conditions, an acceleration of the hydration process may happen. In order to preserve samples as much as possible from carbonatisation, very large surface containers with solid NaOH of analytical grade purity (NaOH aufträger) were initially introduced into the oven. The samples were introduced directly at 105 °C and no temperature gradient program was used. The drying was continued for the specified drying times.

2.1.5. Solvent exchange method

A solvent exchange method was also attempted in this study, but the strong sorption of the organic liquid by the cement paste (as shown by the ^1H NMR results) required the use of relatively high temperatures, at which a still incomplete removal of the organic liquid resulted, and the tests made by gas adsorption showed a very small surface area (<2 m^2/g).

In our opinion the use of organic liquids for exchange introduce additional complications and brings artifacts, which is also compatible with the opinions of Taylor and Turner [27]. For this reason, the solvent exchange method was excluded from the current drying methods comparison study.

2.2. Techniques used for the investigation of drying method efficiency (water removal) and drying implications

2.2.1. Gas adsorption measurements (N_2 adsorption–desorption)

The dried samples prepared by the specified drying methods and their respective specified conditions described above were further investigated by the gas adsorption technique using N_2 as the adsorptive gas, and the results for specific surface areas, porosities and pore size distributions were compared. Nitrogen adsorption and desorption were conducted using an ASAP 2010 apparatus, from Micromeritics. A preliminary study of the precision of the analyzer (ASAP 2010) using a silica/

alumina reference material supplied by Micromeritics showed the standard deviation of the analyzer to be ±1.5 m^2/g for N_2 surface area measurements. Surface areas were calculated by the Brunauer, Emmett and Teller (BET) method over a relative pressure range of 0.05–0.25 on the adsorption branch, and by the Langmuir method, when needed, over the same relative pressure range of 0.05–0.25 again on the adsorption branch. Porosities and pore size distributions were calculated by the Barret, Joyner and Hallenda (BJH) method from both adsorption and desorption branches, also for comparison purposes and for fitting the best results that agreed well with other measurements. From prior work [28] with hardened cement pastes, the outgas level was found also to be a variable affecting the gas adsorption results. For this reason, two outgas levels were investigated with the drying experiments.

2.2.1.1. Aim of outgas. The aim of outgas is to eliminate most of the species physisorbed during storage of the sample (e.g. H_2O vapor in the air, CO_2, etc.), to avoid any drastic change as a result of ageing, sintering or modification of surface functional groups, and to reach a well-defined, reproducible, intermediate state that would be suitable for the proposed experiments (adsorption isotherm measurements). This state can be attained by an appropriate form of vacuum outgas [29].

2.2.1.2. The problem concerning the outgas and the criteria for choosing the outgas vacuum level. Cement paste, even in the "dried state", is a transient reactive adsorbent with its surrounding atmosphere and within itself (hydration is a continuous process as long as there is still water for hydration). The C–S–H gel, which is the main phase of a cement paste, is very sensitive to water removal, as the water participates in its chemical structure. Outgas for cement pastes can be also a "drying" process and not any longer simply a physical desorption of the physisorbed species if it is stronger and longer than is needed to remove these species and to leave the surface "clean" for adsorption. This requires a careful measurement of the mass of adsorbent in its initial state and of the mass change undergone on outgassing—since the reference mass will be that of the outgassed sample, but care must be taken not to change the sample mass by some "chemical" desorption. Therefore, this evacuation must be short and not severe; the pressure in the bulb must not be lower than a few mTorr (mbar) to limit "water desorption" [29]. For this, the first vacuum outgas was chosen to be at the same level as the partial pressure attained by the P-drying method, around 8×10^{-3} Torr (the partial pressure attained by other drying methods is still lower). The subsequent vacuum level was a little lower than the first one, at around 6×10^{-3} Torr (the final vacuum reached by the oil-vacuum pump of the ASAP 2010 apparatus is 5×10^{-3} Torr).

2.2.2. Thermogravimetry measurements

To calculate the relative percentages of the removed water by each drying method,the following formula was applied:

$$\frac{W_0 - W_d}{W_0 - W_i} \times 100\% \quad (1)$$

where W_0—weight of the hydrated cement paste before drying in [g]; W_d—weight of the hydrated cement paste after drying in [g]; W_i—weight of the hydrated cement paste after ignition in [g].

2.2.3. ^1H solid state NMR measurements

In addition, ^1H solid state NMR measurements were carried out to evaluate quantitatively the percentages of remaining water (by integration of resonance signals, H–O–H signal at 5 ppm), and to compare these results with results from thermogravimetry analysis. Measurements were performed on a Bruker DRX 700 spectrometer, applying a magnetic field of 16.44 T with a ^1H resonance frequency of 700.12 MHz. A 2.5 mm sample was used, applying a spinning speed of 30 kHz and a recycle delay of 5 s. Measurements were performed applying the technique of magic angle spinning (MAS). Within all experiments, the 90° pulse length was 2.5 μs. Before the analysis of the spectra could be performed, the background signals had to be eliminated by subtraction. Integration was performed by spectral deconvolution using win NMR. For comparison purposes, the additional spectra of finely milled quartz with "mobile", but still not liquid-like, physically bound water, and of a rehydrated sample with the same water quantity (sample P_2), but dried again, were also obtained. Experiments with the rehydrated sample were performed on a Bruker DSX 300 spectrometer at a magnetic field of 7.05 T. All other parameters were constant. Initially, the sample was mixed with an equivalent amount of water, stored for 10 min at room temperature and finally vacuum evacuated.

3. Results and discussion

3.1. Isotherm types

The hysteresis loops for all isotherms obtained are of type H_3 in the IUPAC classification, with no indication of a plateau at high p/p_0, and, therefore, they should not be regarded as Type IV isotherms (Figs. 2 and 3). Each adsorption branch appears to have the same typical type II character and the desorption branch follows a different path until a critical p/p_0 is reached. Such isotherms, which are named pseudo type II isotherms or II b are given by either non-rigid, slit-shaped pores or assemblages of plate-like particles [29]. The absence of the plateau may be an indication of incomplete mesopore filling. Two kinds of isotherm shapes belonging to the same type II b could be easily distinguished by comparing all the isotherms obtained (Figs. 2 and 4).

3.1.1. Vacuum-treated samples group (large width of hysteresis loop)

Freeze-drying, D-drying, P-drying and Oven-drying for 3 h, (the last only for the outgas level of 8×10^{-3} Torr, Fig. 5) have, as a common feature, a larger width of the hysteresis loop. This adsorption isotherms group is named in this work as vacuum-treated samples (except the 3 h oven-drying at 105 °C). P-drying is also associated with the group above because its isotherm shows the same characteristic as vacuum-treated

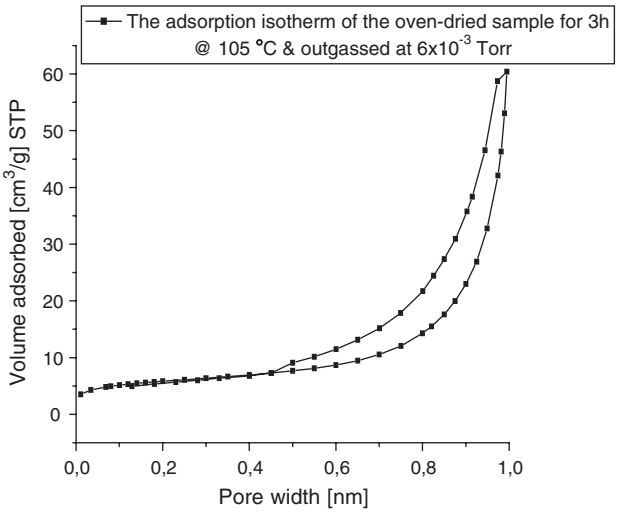

Fig. 2. The adsorption isotherm of the oven-dried sample.

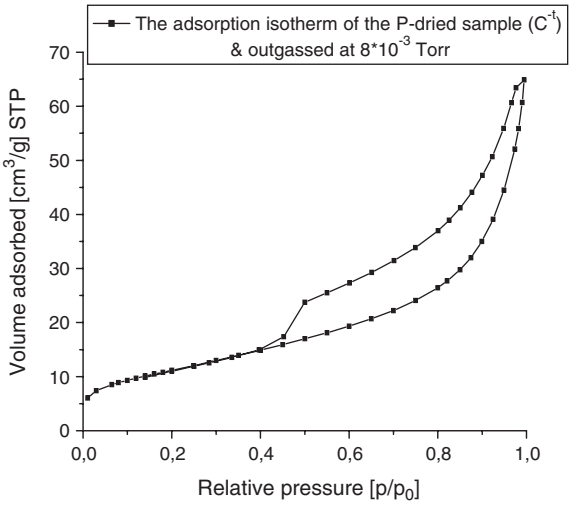

Fig. 4. The adsorption isotherm of the P-dried sample.

samples (Fig. 4). For the isotherm shape similarity between the 3 h oven-drying and D-drying, Beaudoin reports a similar observation [26]; however, in this study, this similarity is conditioned by the vacuum outgas level applied.

3.1.2. Temperature-treated samples group (narrow width of hysteresis loop)

For the vacuum outgas level of 6×10^{-3} Torr, the 3 h oven-dried sample at 105 °C shows now the same characteristic as the 24 h oven-dried sample at 105 °C, having, as a common feature, a narrower hysteresis loop (named here as temperature-treated group, Fig. 2). This narrower loop accounts for a possible pore widening, as the desorption branch follows a path closer to the adsorption branch, and can be interpreted as an easier desorption (the same adsorbate quantity is desorbed at slightly higher relative pressures) in the case of temperature-treated samples (for 3 h oven-dried sample only for the outgas level 6×10^{-3} Torr). As Lippens and De Boer [31] state: "the smaller widths of the hysteresis loops may be caused by deviations in the geometry of the pore model, for example when not very narrow constrictions are present, in tubular pores closed at one end". A similar conclusion can be drawn in this case; a narrower path of the desorption branch may be interpreted as less present narrow constrictions or as mesopore widening, manifested by a relatively easier desorption.

3.2. Specific surface areas and porosities

The specific surface area results and other details are shown for the two outgas levels used in Tables 2 and 3. First of all, in the case of a *C*-value outside the common range of validity or one which is negative, the BET equation cannot be adapted for calculations of the specific surface areas [29]. In these cases, the Langmuir method (monolayer adsorption) fits much better (linearity coefficient 0.999 or better in these experiments), and between the Langmuir specific surface area and the BJH desorption cumulative area, much better agreement results than with the BET method. For the 3 h oven-dried sample at 105 °C and outgassed to 6×10^{-3} Torr, a much better fit results also by the Langmuir method (due to the high *C*-value).

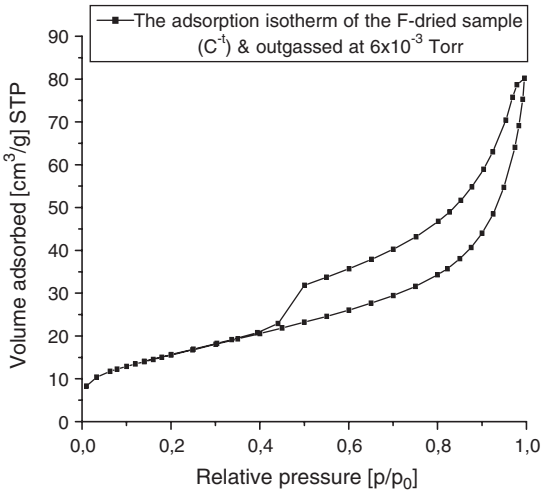

Fig. 3. The adsorption isotherm of the freeze-dried sample.

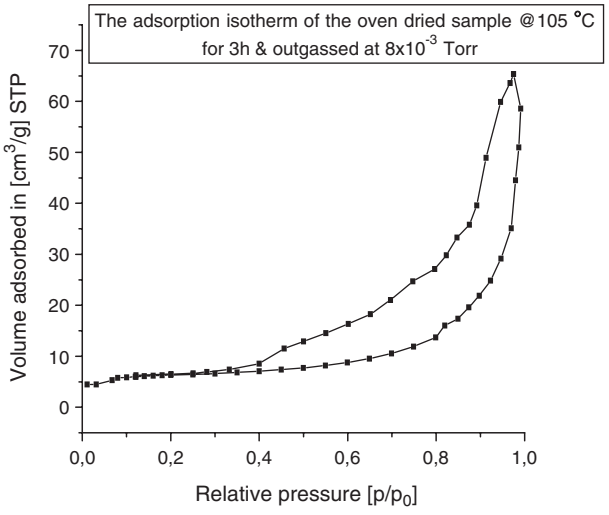

Fig. 5. The adsorption isotherm of the oven-dried sample.

Table 2
Comparison of specific surface areas, micropore areas, volumes and pore widths for samples outgassed at 8×10^{-3} Torr

Sample number	BET area (m^2/g)	*C*-value	Micropore volume (cm^3/g)	Micropore area (m^2/g)	BJH cumulative area (m^2/g)	BJH cumulative volume (cm^3/g)	BET 4V/A D (nm)	BJH 4V/A D (nm)	Langmuir area (m^2/g)
P_1. D-dried 12 h	24	−74	0.01	21	34.94	0.089	9.955	10.18	31.72
P_2. D-dried C^{-t}	51.77	77	–	–	66.387	0.124	7.38	7.486	72.38
P_3. P-dried C^{-t}	40.84	77.6	–	–	53.538	0.1016	7.89	7.596	57.184
P_4. Oven-dried 3 h	21.98	−154	0.059	12.682	35.218	0.1016	12.53	11.539	29.526
P_5. Oven-dried 24 h	29.10	110	0.0006	1.787	42.283	0.1135	11.38	10.735	40.434
P_8. F-dried C^{-t}	56.9	73.8	–	–	69.436	0.1262	6.96	7.27	79.67

The vacuum-treated samples represent a higher specific surface area in every case than the temperature-treated ones (oven-dried samples at 105 °C). Inside the vacuum-treated group the freeze-dried (F-drying C^{-t}) samples represent the highest specific surface areas for both outgas levels, followed by D-dried (C^{-t}) and P-dried (C^{-t}) samples (the symbol C^{-t} stands here for drying until 0.001 g/g paste per day of drying weight loss rate was reached).

3.3. The microporosity assessment and vacuum outgas level influence

The total volume and microporosity area (pores <2 nm width) can be assessed only quantitatively without any pore size distribution, by using the so-called "t-plot" method (V_{ads}-t) [31]. The Kelvin equation cannot be applied to these pore sizes [29,31]. By applying this method, the 12 h D-dried sample, the 3 h oven-dried sample at 105 °C and the 24 h oven-dried sample at 105 °C surprisingly represent some "microporosity" at both outgas levels (8×10^{-3} and 6×10^{-3} Torr). (In every case, for the first linear part of the t-plot the linearity coefficient was between 0.95 and 0.99.) It is also interesting that these microporosities are present only for the relatively short drying time of 12 h D-drying and short time, fast drying methods, namely the 3 h oven-drying and the 24 h oven-drying at 105 °C, and are absent for the vacuum-treated sample group (except the 12 h D-drying). Lawrence et al. also represents the same opinion by mentioning that micropores are present in rapidly dried pastes that have been cured at room temperature, but are possibly absent from slowly dried systems [32]. As expected, there is an influence of the vacuum outgas level applied for some of the samples. The vacuum outgas level affects mainly the results for the 12 h D-drying, by increasing the total specific surface area value and by reducing drastically the area of the few "micropores" present (the micropore volume is only 0.01 cm^3/g from the total volume of 0.089 cm^3/g). The 12 h D-drying method represents the highest "microporosity" that is drastically reduced at the outgas level of 6×10^{-3} Torr, followed by the 3 h oven-dried sample, affected also by the vacuum outgas level. Leaving for later on the discussion of these represented "microporosities", from theoretical considerations it can be said, however, that the microporosity findings are doubtful as long as some preconditions are fulfilled. The cement paste system is a highly "non-ideal" sorption system (Section 2.2.1.2); classical equilibrium is difficult to envision for this system [33]. If this method can be successfully used for assessment of microporosity, then the need for a reference non-porous hardened cement paste would be the main condition for applying accurately quantitatively the "t-plot" method to dried cement paste samples. The negative *C*-value of the BET equation (the reason is not well understood), in the case of 12 h D-drying and 3 h oven-drying at 105 °C (outgassed to 8×10^{-3} Torr), is also a point of doubt. An indication for the possible presence of micropores is a high *C*-value as a representation of the enhancement of initial adsorption energy due to the significantly increased adsorbent–adsorbate interactions [29]. But on the other hand, a large disagreement between:

(a) the total specific surface area and the BJH cumulative specific surface area (as shown in Table 2) [30],
(b) the total specific surface area and the surface area calculated by application of the t-plot method, and
(c) a downward deviation from linearity after the first linear part at low relative pressures [31] favor the opinion for the possible presence of some microporosity together with "meso" or macropores (Fig. 6). A downward deviation from linearity at low relative pressures indi-

Table 3
Comparison of specific surface areas, micropore areas, volumes and pore widths for samples outgassed at 6×10^{-3} Torr

Sample number	BET area (m^2/g)	*C*-value	Micropore volume (cm^3/g)	Micropore area (m^2/g)	BJH cumulative area (m^2/g)	BJH cumulative volume (cm^3/g)	BET 4V/A D (nm)	BJH 4V/A D (nm)	Langmuir area (m^2/g)
P_1. D-dried 12 h	39.023	95	0.00033	1.698	49.47	0.109	7.97	8.816	54.334
P_2. D-dried C^{-t}	52.15	73.5	–	–	66.75	0.123	7.395	7.37	73.06
P_3. P-dried C^{-t}	42	74.8	–	–	53.56	0.1017	7.84	7.54	57.12
P4. Oven-dried 3 h	20.7	312	0.0025	5.836	28.93	0.0938	12.59	12.56	28.43
P_5. Oven-dried 24 h	28.105	115.73	0.0007	1.82	40.68	0.10	11.375	10.71	40.42
P_8. F-dried C^{-t}	58.94	75	–	–	69.484	0.132	6.915	7.264	79.683

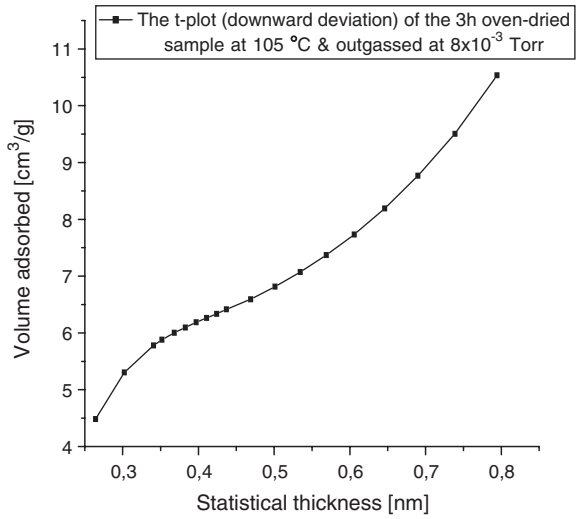

Fig. 6. The t-plot case from an oven-dried sample.

cates that micropores become filled by multilayer adsorption at low relative humidity, reducing the surface available for continued adsorption [29]. Lippens and DeBoer [31] and De Boer et al. [34] attribute this kind of deviation to the blocking of micropores by the growing adsorbed layer at increased relative pressures, and after these the extrapolation of the second straight line to zero relative pressure would yield a measure of the volume of the adsorbate in the previously blocked micropores. In gas adsorption theory, the opinion is favored that primary filling of micropores (ultramicropores) by N_2 at 77 K begins at $p/p_0 < 10^{-5}$ and is complete at $p/p_0 = 10^{-2}$, and that supermicropores and very narrow mesopores (0.7–1.8 nm), which are present in slit-shaped, sheet-like nanostructures (as in the case of cement microstructures), are filled in the range $>0.01 p/p_0$, which corresponds to 7.760 mTorr (easily attained by the ASAP 2010 apparatus). Also an enhancement of adsorbent–adsorbate interactions can be expected only for the ultramicropore range (pores <0.7 nm width), and there can be no significant enhancement of initial adsorption energy in supermicropores and very narrow mesopores of larger pore widths (0.7–1.8 nm) [29]. In a mesoporous solid (2–50 nm) containing also some micropores, the initial stage of N_2 adsorption is by monolayer adsorption on the walls of supermicropores, followed by the formation of a quasi-multilayer, until pore filling is complete at around $p/p_0 = 0.4$. The existence of micropores (0.7–1.8 nm, or 2–4 molecular diameter of water) would give rise to surface phenomena, other than adsorption e.g. molecular bridging. However in light of all these facts (pro and against), the results concerning the presence of "micro-porosities" can be taken as a qualitative indication (and the possibility of overestimation should be also accounted for, as it is argued later). For the rest of the vacuum-treated samples group (without 12 h D-drying), and for the 24 h oven-dried sample at 105 °C there is almost no influence of the second vacuum outgas level, and this is expected, since, at the end of the drying time a relative humidity lower or equal to the chosen vacuum outgas is reached (for oven-dried samples, the final relative humidity after drying was not controlled). Even though the oven-drying methods and the 12 h D-drying method show some micropores, the total specific surface areas are still much smaller than the specific surface areas obtained by the other drying methods. By a stronger and prolonged outgas (5×10^{-3} Torr), the 12 h D-dried sample (P_1) gave nearly the same results as the D-dried (C^{-t}) sample accompanied by a gradual "micropore" area decrease, whereas the 3 h oven-dried sample at 105 °C did not show any considerable difference of total specific surface area, except for a decrease in micropore area, as shown in Table 4. There is a perfect agreement for the non-micropore, representing drying methods with the hysteresis-loop type, "t-plot" character and assumed pore geometry, as concluded by Lippens and De Boer [31]; ink-bottle or slit-shaped pores give generally type B hysteresis (H_3 IUPAC classification); they represent linear or downward deviations (at high relative pressures $>0.8 p/p_0$), and this character of the t-plots is an indication that no micropores are present. This is also the case for F-drying C^{-t}, D-drying C^{-t} and P-drying C^{-t} methods, and the t-plot case is shown in Fig. 7.

3.4. Thermogravimetry results

As mentioned in the Experimental section of the investigation methods, additional results are supplied by thermogravimetry analysis, represented graphically in Fig. 8. These results are calculated using formula (1) and are based on weight differences after drying and ignition at 1005 °C. Comparing the percentages of the removed water with the resulting specific surface areas, it can be said that a higher water removal does not result in every case in a larger specific surface area and

Table 4
Comparison table for the influence of the outgas level at samples P_1 and P_4

Sample number	BET area (m^2/g)	*C*-value	Micropore volume (cm^3/g)	Micropore area (m^2/g)	BJH cumulative area (m^2/g)	BJH cumulative volume (cm^3/g)	BET 4V/A D (nm)	BJH 4V/A D (nm)	Langmuir area (m^2/g)
P_1. Outgas $8*10^{-3}$ T	24	−74	0.01	21	34.94	0.089	9.955	10.18	31.72
P_1. Outgas $6*10^{-3}$ T	39.023	95	0.00033	1.698	49.47	0.10903	7.97	8.816	54.334
P_1. Outgas $5*10^{-3}$ T	51.68	77	–	–	61.042	0.1097	6.31	7.18	72.375
P_4. Outgas$8*10^{-3}$ T	21.98	−154	0.059	12.682	35.218	0.1016	12.53	11.539	29.526
P_4. Outgas $6*10^{-3}$ T	20.7	312	0.0025	5.836	28.93	0.0938	12.59	12.56	28.43

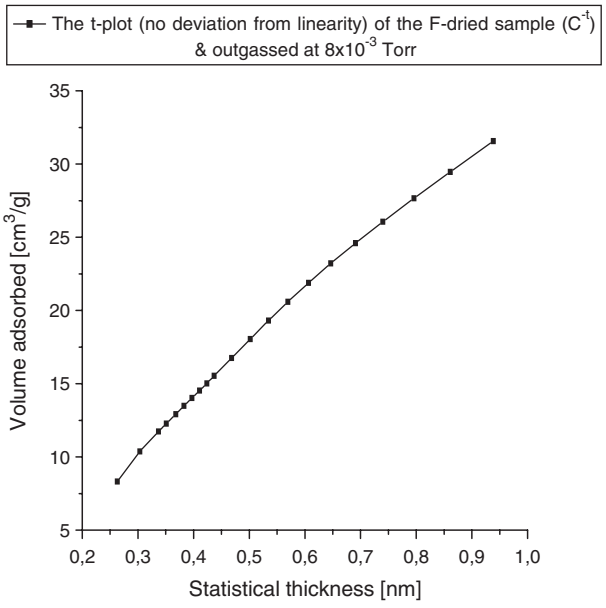

Fig. 7. The t-plot case from an F-dried sample.

more accessible porosity. In the case of D-dried samples (D-drying 12 h–D drying C^{-t}) an increase in surface areas results by stronger drying (drying plus outgas for 12 h D-Drying) until a maximum value is attained by this method, namely around 52 ± 1.5 m^2/g. The specific surface areas for the F-dried samples appear the largest, even though the relative percentage of the removed water is not the highest, possibly due to the well known reason of a capillary effects softening. For the group of temperature-treated samples (oven-dried samples at 105 °C), the relative percentages of the removed water are slightly higher than for the other drying methods, but the surface area results are considerably smaller than for the group of vacuum-treated samples. Such results can be interpreted as a possible pore collapse, or at least pore alteration, from these drying methods (the isotherm shape supports this conclusion, as mentioned above). It is necessary to mention that the resulting percentage of removed water for the 12 h D-drying method is calculated before outgas, and that a considerable weight decrease after a very long outgas time has occurred as shown in Table 5 (the calculated, new relative percentage of the removed water after outgas to 8×10^{-3} Torr is still below of all the calculated percentages of the removed water after drying and prior to outgas, shown in Fig. 8). The weight losses for the other methods at this outgas level were equal to or less than 0.001 g/g of outgassed sample, and are not shown. From the very small percentage of the removed water after drying and prior to outgas, and the considerable weight decrease after outgas, it can be said that a considerable "drying" has happened for the 12 h D-dried sample during the outgas process. Not all of the calculated "hydraulic" diameters shown in Tables 2 and 3 and also in Table 4 are reliable, because, for "micropore"-indicating samples (except for the 24 h oven-drying sample at 105 °C and outgassed to 6×10^{-3} Torr), the Langmuir specific surface areas should be taken into account rather than BET specific surface areas. In any case, a larger specific surface area is accompanied by a smaller mean "hydraulic" radius, and a shifting of pore width to finer pores results (taking into account only the mesopores region between 2 and 50 nm pore width) (Figs. 14 and 16).

3.5. ^1H solid state NMR measurements

Additional results for the quantities of the "remaining" water are supplied by ^1H solid state NMR measurements, depicted in Figs. 9 and 10. An "*" within the spectra represents spinning side bands due to the applied MAS technique, which results in an improved spectral resolution, even for rigid samples. Before the analysis of the spectra could be performed, the background signals had to be eliminated by subtraction. The spectrum P_6 is the spectrum of the strongly bound organic solvent (alcohol) sample, which was excluded from further investigations of the drying exchange method as mentioned above. The peak signal resonances represent the H–O–H signal at 5 ppm and the O–H signal at 1 ppm. There exists a small difference between the peaks at 5 ppm, accounting for some small differences in the remaining water quantities. To obtain quantitative information about the remaining water quantities, an integration was performed by spectral deconvolution using the win NMR technique. The results of such integration, even though with a relatively high error margin (±5%), give an approximate idea of the "non-removed" water quantities (Table 6). The results agree very well with the thermogravimetrical results for the 12 h D-dried sample and for 24 h oven-drying at 105 °C. The other results of the "remaining" water quantities differ very little from each other,

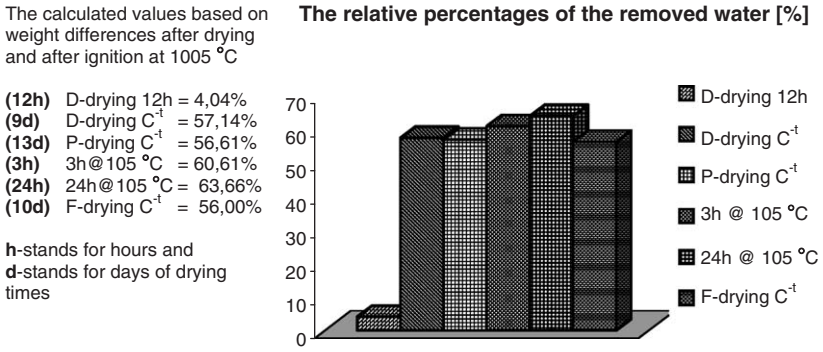

Fig. 8. The calculated values for relative percentages of the removed water (before outgas).

Table 5
Table of the weight change due to outgas

Drying method used	Vacuum outgas level	Weight before outgas (g)	Outgas time (h)	Weight after outgas (g)
D-dried 12 h	Outgas $8*10^{-3}$ T	0.36	46	0.28
D-dried C^{-t}	Outgas $8*10^{-3}$ T	0.36	8	0.36
P-dried C^{-t}	Outgas $8*10^{-3}$ T	0.30	13	0.30
Oven-dried 105 °C 3 h	Outgas $8*10^{-3}$ T	0.34	11	0.34
Oven-dried 105 °C 24 h	Outgas $8*10^{-3}$ T	0.34	8	0.34
F-dried C^{-t}	Outgas $8*10^{-3}$ T	0.33	10	0.33

and also agree well with the results from thermogravimetry analysis (taking into account the relative error of ±5%). There is no great difference to be observed comparing the ^{1}H NMR spectra of the 24 h oven-drying at 105 °C method and the rest of the drying methods, giving evidence that there is no "absolute drying", as still there are traces of molecular water present even after strong drying, but the structural and physical water ratios still cannot be distinguished. However, the water remaining after drying is "immobilised" water, as compared to that which is relatively "mobile", physically adsorbed on the external surface of inert "non-porous" quartz grains, as shown in Figs. 11 and 12. Our conclusions for the state of water are also consistent with those of others [15]. The water left is non-liquid water and it is strongly bound non-condensed molecular water, present maybe as interlayer water and water molecules at the "kinks" of irregular sheets alignment, as in the model suggested by Feldman and Sereda and modified by Daimon et al. [15], and water strongly retained by the smallest, slit-shaped gel micropores. Calculations of the interlayer space (based on a layered model) of the cement structure, using the differences on the surface area and pore volume between water and nitrogen [15], give a value of 0.28–0.32 nm with water–cement ratio ranging from 0.4 to 0.5. Interlayer space of this dimension would contain only a single layer of water molecules. The quantities left vary possibly from structural interlayer water of a partly collapsed-altered structure for the 24 h oven-dried samples at 105 °C (the opinion is favored that 24 h oven-drying at 105 °C removes "completely" the non-bound water), by some few molecules, gel water (at pores <2 nm the water cannot condense), differing in quantity for all the samples depending on drying efficiency.

3.6. Porosities and pore size distributions interpretation

The decision as to which branch should be taken for pore size analysis is still today an open discussion for gas adsorption researchers, and it can be said also that neither the adsorption (due to delayed menisci formation) nor the desorption branch (due to delayed evaporation or pore emptying) will represent the real equilibrium, and as a consequence, it should not be expected that the calculations will represent perfectly the pore size distributions (PSD). However, for comparison purposes, the supplied results are of very great significance. Pore size distributions were calculated from both adsorption and desorption branches, and for both vacuum outgas levels, and an attempt was made to try to correlate the results for specific

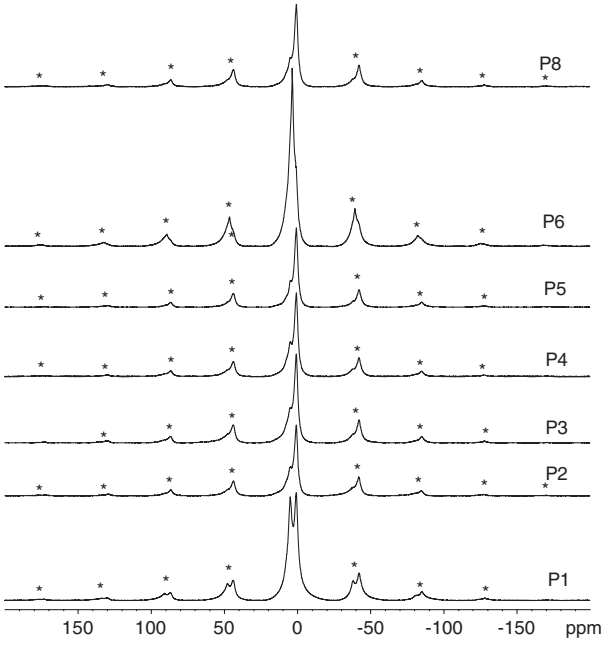

Fig. 9. ^{1}H NMR-MAS spectra of the dried samples and prior to outgas.

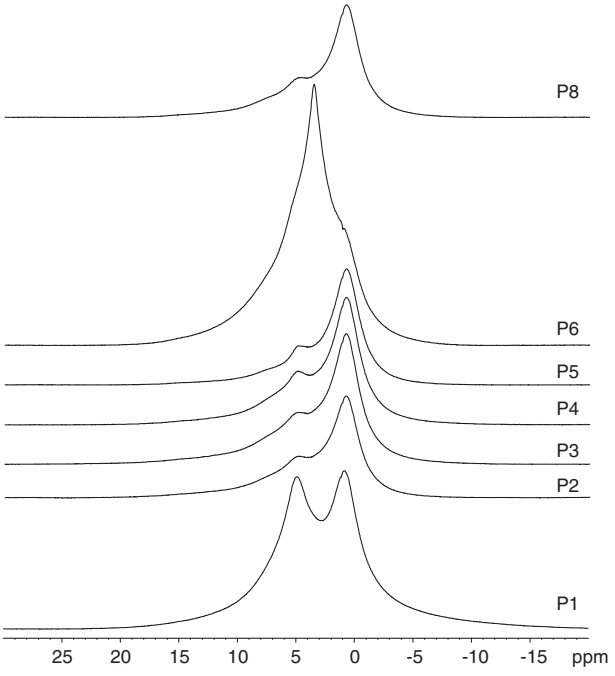

Fig. 10. The main signals of the previous spectra (Fig. 9), H–O–H signal at 5 ppm, and O–H signal at 1 ppm.

Table 6
The integration results for the relative percentages of non-removed water by win NMR spectral deconvolution

Sample number	P_1. 12 h D-dried	P_2. D-dried C^{-t}	P_3. P-dried C^{-t}	P_4. 3 h at 105 °C	P_5. 24 h at 105 °C	P_6. Solvent exchange	P_8. F-dried C^{-t}
Signal at 5 ppm (%)	54	31	28	29	18	35	26

surface areas with those of the relative removed water quantities and porosities. Pore sizes distributions are based on the Kelvin equation, its applicability being at around the 2–50 nm pore size range, and the represented plots leave out the results for "microporosities" (here supermicropores and very narrow mesopores 0.7–1.8 nm). Referring to the BJH cumulative surface areas (Tables 2 and 3), the calculations based on the desorption branch overestimate the specific surface area and give values equal to the Langmuir specific area, even though the micropore areas are not included by the BJH cumulative pore areas calculation. In this case, the BJH adsorption cumulative pore areas agree much better with BET areas (even though the BET areas do not represent always the real specific surface areas, as for 12 h D-drying, 3 h and 24 h oven-drying at 105 °C). These suggest that the pore size distributions (PSD) would better be reflected by referring to the adsorption branch, whereas for the F-drying C^{-t}, D-drying C^{-t} and P-drying C^{-t}, both branches would represent similar results with only small shifts (Figs. 13 and 14 or 15 and 16). The conclusion that more removed water does not always result in more accessible surface areas and porosities is supported also by adsorption BJH pore size distribution (PSD) comparison plots (Figs. 14 and 16), and, especially, by the cumulative pore volumes and cumulative pore area distributions (Figs. 21–24). The cumulative pore volumes and cumulative pore area plots stand generally above the others for F-drying C^{-t}, D-drying C^{-t} and P-drying C^{-t} at around the 2–4 nm range, but beyond this range there are already 24 h oven-drying, 3 h oven-drying and 12 h D-drying plots standing generally slightly above the first mentioned plots, up to around 50 nm. There is also an artificial pore width shifting to coarser pores, resulting from the incomplete water removal 12 h D-drying method, and a real pore width shifting for the strongest drying methods, namely 24 h oven-drying and 3 h oven-drying at 105 °C. The effects of vacuum outgas levels are shown in Fig. 17; for the 12 h D-dried sample more removed water due to drying (drying plus outgas) gives access progressively to finer pores, approaching more and more the results given by D-drying C^{-t} and outgassed to 6×10^{-3} Torr. The outgas level effects for 3 h oven-dried sample (Fig. 18) are not the same as for the 12 h D-dried sample; the pore widths are shifted to slightly larger (coarser) ones, also giving support to the conclusion of a pore size widening. The desorption plots of the vacuum outgas levels influence in Figs. 19 and 20 are also shown, only for comparison purposes with the results from adsorption branch. As can be seen from the PSD plots of the micropore-representing samples (except 24 h oven-drying at 105 °C), a large difference exists between the two different distributions, whether referred to the adsorption or to the desorption branch (Figs. 13–16). The pore width peaks are shifted to smaller diameters around 3–3.5 nm (3.5–4 nm for 24 h oven-drying at 105 °C) for the outgas level 8×10^{-3} Torr and PSD referring to the desorption branch. The PSD referring to the adsorption branch indicate a shift at around 6.5–7 nm pore volume maximum for the same outgas level of 8×10^{-3} Torr, which seems to be more probable by agreeing well with the results for specific surface areas and porosities (Figs. 21–24). For the non-micropore-representing samples, there is a much better agreement of both distributions with each other; the main pore volume peaks for the non-micropore-representing samples are localised at around 3.5–4 nm referring to the desorption branch, and at around 2–2.5 nm (3 nm for P-drying C^{-t}) referring to the adsorption branch. The trend is clear that the F-drying C^{-t}, D-drying C^{-t} and P-drying C^{-t} remove water quantities slightly below the 24 h oven-drying method, which removes the largest water quantity. Inside this group, as more water is removed, finer pores are accessed, but probably still the gel pores cannot be accessed (pore widths <2 nm) or a

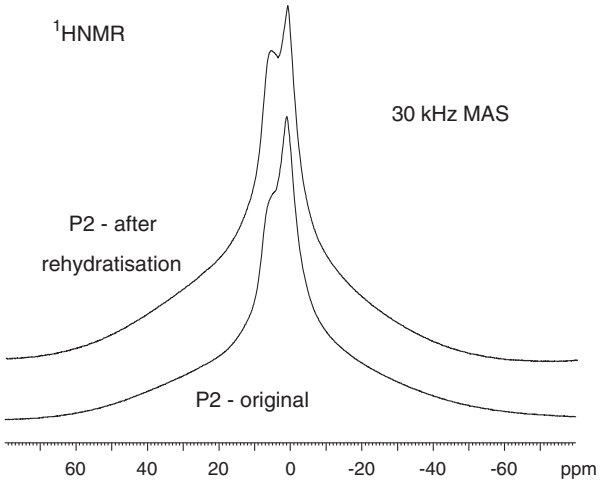

Fig. 11. ^{1}H NMR spectrum of "immobilised" water.

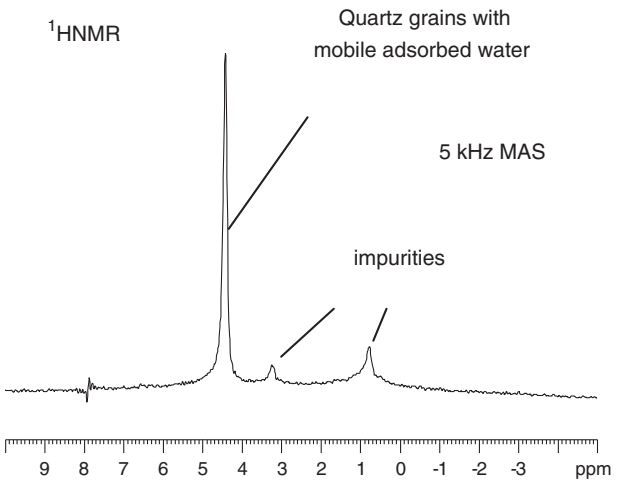

Fig. 12. ^{1}H NMR spectrum of relatively "mobile" water.

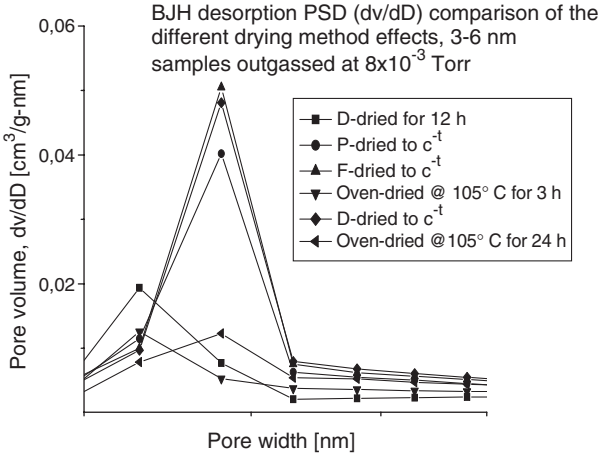

Fig. 13. BJH desorption PSD comparison for all samples outgassed at 8×10^{-3} Torr.

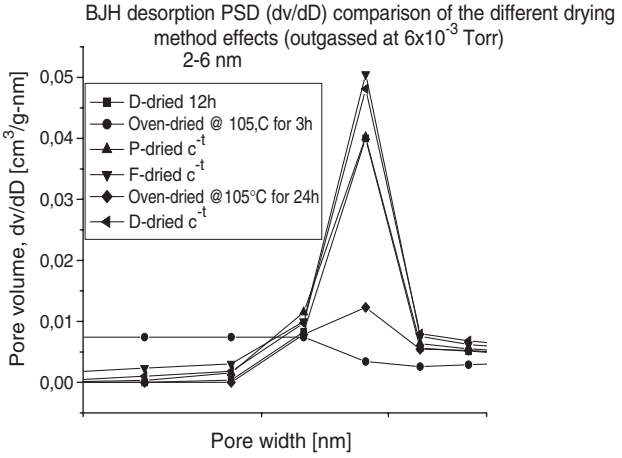

Fig. 15. BJH desorption PSD comparison for all samples outgassed at 6×10^{-3} Torr.

micropore collapse should be accounted for as discussed below. As the trend in water removal pores size accessibility is obvious, the real mesopore width peaks may be localised between 2 and 4 nm for the F-drying, D-drying and P-drying C^{-t} (vacuum-treated samples without 12 h D-drying), and between 3 and 7 nm for 12 h D-drying, 3 h oven-drying and 24 h oven-drying at 105 °C, based on the above-mentioned fact that both branches do not give a perfect "picture" for the PSD. Concerning the absence of microporosities for F-drying C^{-t}, D-drying C^{-t} and P-drying C^{-t} (vacuum-treated group), two possibilities can be assumed;

(a) These methods are able to dry the samples relatively well (concerning water removal and preservation inside 2–50 nm), but possibly still are not able to give complete access to the gel micropores (<2 nm), as no measured microporosity results, or;
(b) As favored by other authors, namely Garci Juenger and Jennings [18] and Gimblett et al. [28], the D-drying C^{-t} method removes all of the non-bound water or physically bound water and, moreover, as stated by Skalny and Odler, "one cannot remove the physically adsorbed water without removing also a part of chemically bound water" [35]. In other words, if the D-drying method C^{-t} is able to remove "completely" the water from the capillary and gel pores, there still exists the possibility that some structural water is also removed, together with that which is physically bound. As the relative percentages of the removed water (until a very small, constant weight loss rate is reached), differ very little (always speaking of vacuum-treated samples without 12 h D-drying), a possible partial pore collapse in the very fine gel pore range (<2 nm) should be accounted for, also for this sample group. Whereas the oven-drying methods, by removing the highest quantities of water (more than the D-drying C^{-t} sample), may give access to the gel porosity, but being strong drying methods (gradient stresses generated) and using high temperatures can alter the microstructures by reorganisation (pore widening), accompanied by a partial collapse at the same time. Furthermore, even though both drying method groups might cause pore collapse (especially gel pore collapse),

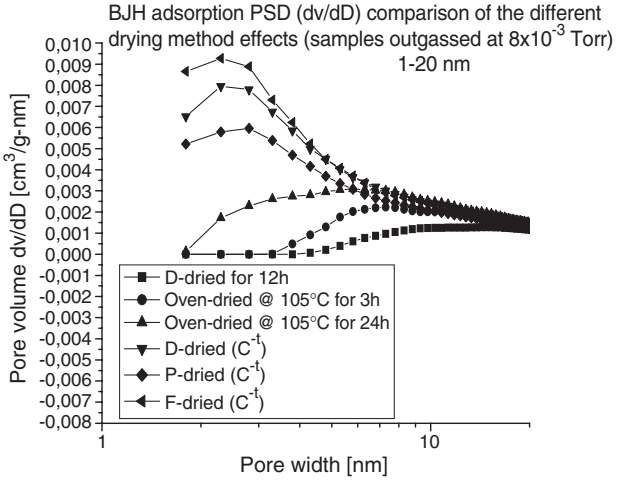

Fig. 14. BJH adsorption PSD comparison for all samples outgassed at 8×10^{-3} Torr.

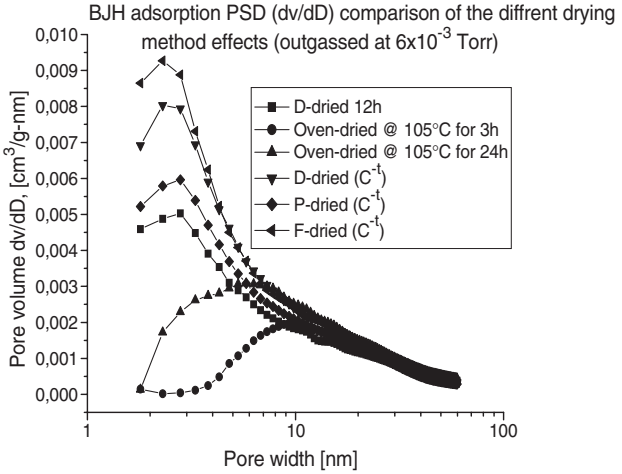

Fig. 16. BJH adsorption PSD comparison for all samples outgassed at 6×10^{-3} Torr.

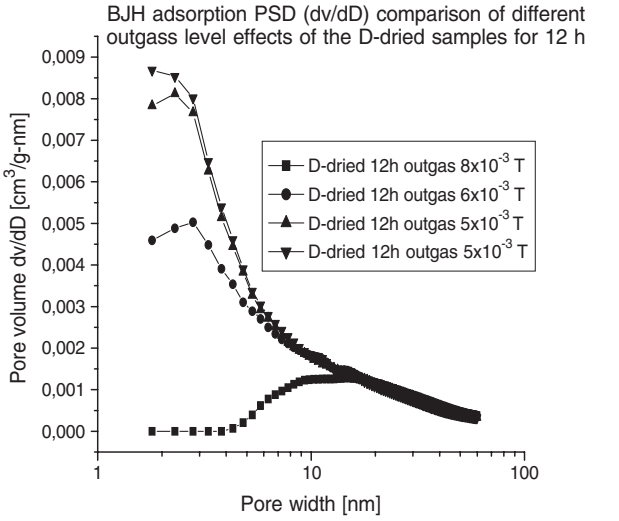

Fig. 17. BJH adsorption PSD comparison for 12 h D-dried samples for different outgas levels.

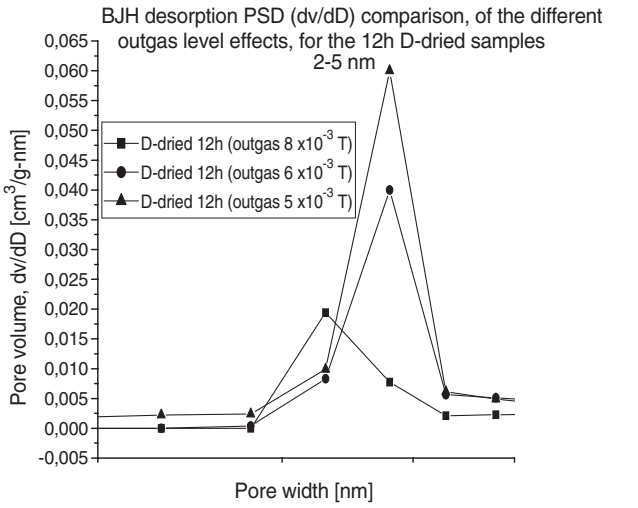

Fig. 19. BJH desorption PSD comparison for 12 h D-dried samples for different outgas levels.

the influence might be different, as some very few microporosities still result from the temperature-treated group. Concerning the represented "micropores", a possible explanation would be that 12 h D-drying probably measures the very narrow entryways or "collars" resulting from the strongly bound, non-structural remaining water molecules. On the other hand, due to some pore blockages, the possibility of an overestimation should also be accounted for (an artificial downward deviation of the t-plot), especially for the outgas vacuum level of 8×10^{-3} Torr. As suggested also by Diamond, the incomplete water removal likely leaves plugs or residual water in the narrowest choke points, which may induce complete pore blockage in some areas of the paste [36]. This is the situation for the "incomplete" water removal method namely 12 h D-drying. The residual water, in the narrowest choke points, induces a partial pore blockage and also prevents at a certain extent access of N_2 molecules, resulting in low specific surface area values. This assumption, which seems very probable, gives an explanation for the resulting "micropores" (supermicropores and very narrow mesopores 0.7–1.8 nm) for the 12 h D-dried samples. Even though the micropores have the highest specific surface area, one should not expect a very high total specific surface area for the 12 h D-dried sample as the volume of the "micropores" present (the so-called micropores which are not micropores but only very narrow entryways created artificially by the remaining water traces) is very small, and almost negligible. A more prolonged drying time logically removes more water from the pores; this additional removed water causes the "choke" points to open and the narrow "collars" to widen to some extent, shifting the resulting pore widths at relatively larger diameters. In this way, as shown by PSD comparisons for different outgas levels for the 12 h D-dried samples (Fig. 17) and from the non-micropore-representing samples group (Fig. 16), more removed water permits more

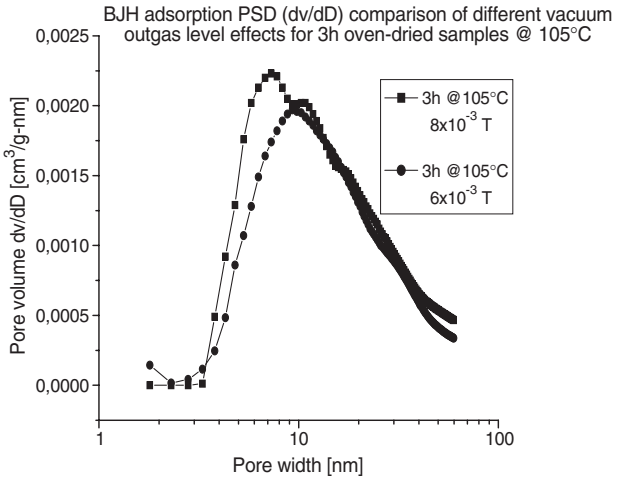

Fig. 18. BJH adsorption PSD comparison for 3 h oven-dried samples for different outgas levels.

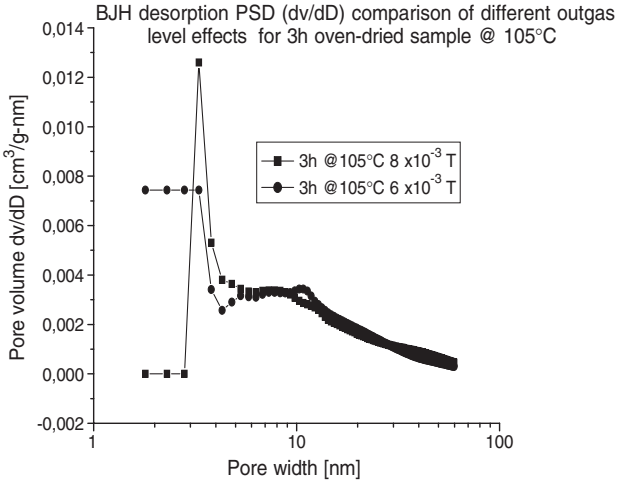

Fig. 20. BJH desorption PSD comparison for 3 h oven-dried samples at 105 °C for different outgas levels.

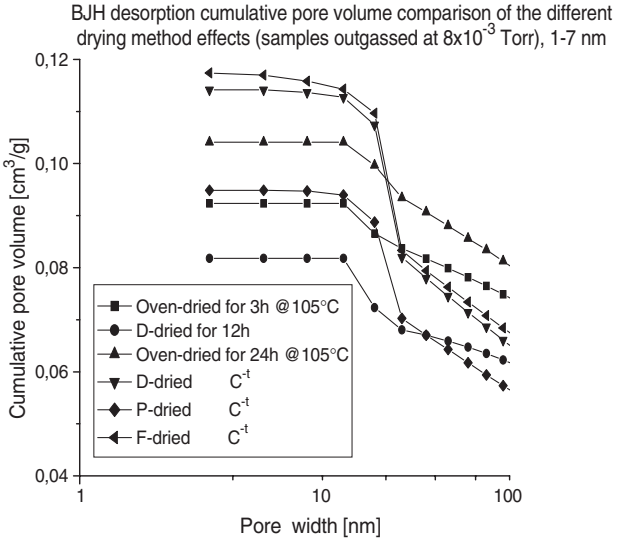

Fig. 21. Desorption cumulative pore volume comparison for outgas level 8×10^{-3} Torr.

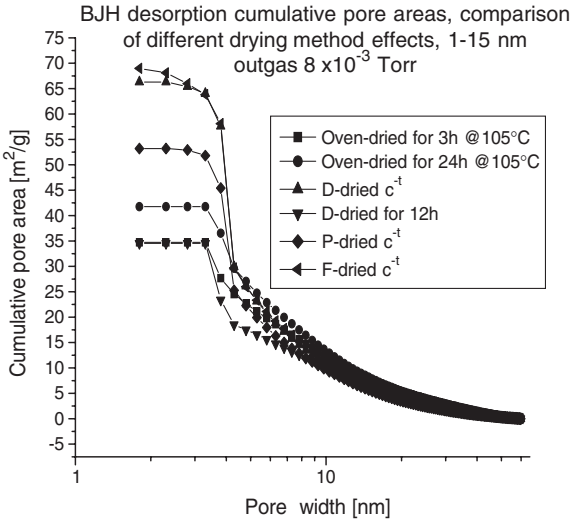

Fig. 23. Desorption cumulative pore areas comparison for outgas level 8×10^{-3} Torr.

access to N_2 molecules, resulting in larger specific surface areas, and accompanied by more pore volume and a drastic decrease of the "microporosity" in the case of 12 h D-drying, due to a progressive decrease of the number of "choke points", and to the widening of the water "collars". For the oven-drying methods, the fact that a lower surface area results, instead of a larger one, as compared to the rest of the drying methods with more removed water, can be interpreted as a possible structural alteration. Also, with a stronger outgas, there is neither an increase nor "apparent" decrease in surface area values, except for a reduction in micropore area, as for the 3 h oven-dried sample at 105 °C (micropores are the most sensitive to the drying). It is evident that all the drying methods used here affect or access the microstructures (mainly C–S–H gel) in different ways, and, if the argument of point "b" more than that of point "a" is accepted, then it can be concluded that both of the drying method groups cause a pore collapse, especially micropore collapse, but in different ways and to different extents. The drying rate possibly may have its effects, as, for shorter drying times, some microporosity results. The attempt to completely remove the "non-structural water" is always accompanied by more microstructural implications. It seems likely that oven-drying alters the microstructure by reorganisation and some pore collapse, and there is a certain point beyond which the structure tends to resist additive collapse; after this point there is no longer a surface area decrease. A maximum surface area value also exists (for this hydration degree) attained by F-drying method, and the surface area increases slowly with more removed water inside the vacuum-treated samples group, and, after reaching this maximum, decreases again by more water removal, until it reaches the minimum with the oven-dried samples, and keeps nearly constant at this point (under these experimental

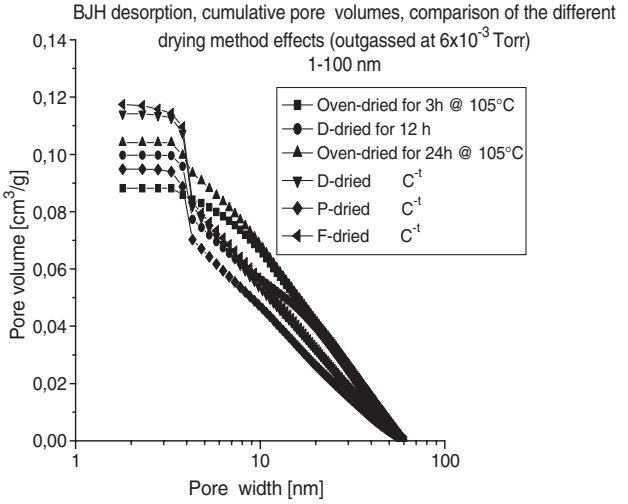

Fig. 22. Desorption cumulative pore volume comparison for outgas level 6×10^{-3} Torr.

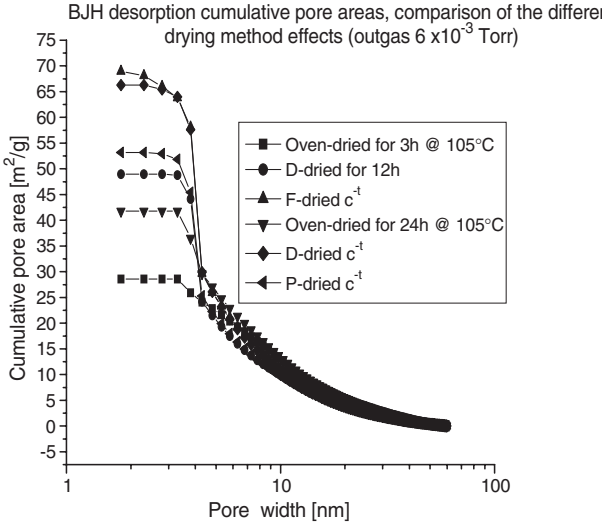

Fig. 24. Desorption cumulative pore areas comparison for outgas level 6×10^{-3} Torr.

conditions). Based on the fact that as for the minimum water quantity removed (12 h D-drying outgas 8×10^{-3} Torr) and for the maximum water quantity removed (24 h oven-drying at 105 °C) the surface area results are almost the same (29.10 and 31.72 m^2/g), it can be concluded that a minimal surface area value exists around 30 m^2/g. Therefore, under these experimental conditions, the hydration degree, $\alpha = 0.75$, and w/c ratio = 0.45 depending on the drying method used, the specific surface area for the cement paste varies between 30 and 60 m^2/g. The most probable C–S–H model that would justify the interpretation of all these results would be a structure made up of irregular primary small size units (2–5 nm) which may not be necessarily spherical as in the Jennings–Tennis model [12], but instead elongated chains. These primary units would form the secondary particle assemblages ranging between 10 and 20 nm diameter sizes by clustering together. Similar to the Feldman–Sereda [6] model, a layered structure of around 0.28–0.32 nm space between sheets would result for the primary units, but the interlayer space would be here in direct contact to the larger entrances to interspaces, gel micropores, between the primary irregular C–S–H units. This is also compatible at a certain extent with a model of creep mechanism proposed by Feldman [37]. The presence of sorbed and bridging water molecules between the primary units should also be possible as in the Munich model [11], affecting in this way the bonding strength of the clusters. The interlayer space in this situation should not be considered as the real gel pore area.

4. Conclusions

A comparison concerning the implications and efficiency in removing only the non-bound water and in microstructure preserving for some typical drying methods used for cement pastes was conducted in this study. The F-drying C^{-t} method (improvised in this study) gives the largest surface area results, confirming the well known fact of capillary softening effects due to sublimation-evacuation. The F-drying C^{-t}, followed by the D-drying C^{-t}, method gives the largest specific surface area values, even though the relative percentages of the removed water are not the highest, but no microporosity results. Contrary to the above-mentioned drying methods, the temperature-treated samples, namely 3 h oven-drying at 105 °C and 24 h oven-drying at 105 °C, represent some microporosity (varying with the vacuum outgas level applied), even though the specific surface areas are well below those represented by those first mentioned. Two main explanations were introduced for such observations, and the argument of point "b" seems more probable (judging from ^1H NMR spectra and the relative removed water quantities). Under these conditions, both groups, namely vacuum-treated samples without 12 h D-drying (F-drying C^{-t}, D-drying C^{-t} and P-drying C^{-t}) and temperature-treated samples (3 h and 24 h oven-drying) may also be able to remove different quantities of the water retained in the gel pores. A possible micropore collapse may occur in both groups of the drying methods, but to different extents, depending on the quantity of the removed water, drying rate, prolongation and reorganisation due to temperature treatment. However, as long as one cannot distinguish between the chemical structure and the strongly physically bound water, nothing can be said for sure as to whether the non-microporosity for the prolonged vacuum-treated samples is due to small gel pore collapse-alteration or due to the lack of water removal from the very small gel pores. For the oven-dried samples, it is very probable that the resulting microporosity is not the original one of the non-disturbed gel microstructures, but rather a microporosity resulting after a rearrangement of the microstructures due to the temperature treatment. This idea is supported by the well known fact that the small gel pores are the most sensitive to capillary effects, and in the case when a pore alteration at around 2–50 nm range exists, it would be not very logical to assume that these microporosities are the original ones, which is an internal characteristic of the C–S–H gel. Concerning the short time version of the D-drying method, namely 12 h D-drying, an incomplete water removal exists and there is no water removed from the very small gel pores (<2 nm), and no access for N_2 molecules to measure the real gel micropores. The represented "microporosity" can result mainly from the narrowed "collars" of the strongly bounded non-structural water, and as an artefact from the contribution of the "t-plot" downward deviation, due to a partial pore blockage caused by the remaining water molecules. All the micropores represented here (if the t-plot method can be applied) are supermicropores and very narrow mesopores in the range 0.7–1.8 nm, suggested by the relative pressure range used during gas adsorption measurements. With reservations concerning the microporosity range or gel porosity, it can be said, however, that, inside the accepted range of Kelvin-equation applicability, namely around 2–50 nm, the F-drying method C^{-t} used in this study gives a more real "picture" for the microstructure, and D-drying method C^{-t} gives slightly worse results. For the conditions of these experiments, hydration degree and w/c ratio, a minimal specific surface area exists of around 30 m^2/g, measured by the "worst" drying methods, namely by the "incomplete" water removal method of 12 h D-drying and outgas level of 8×10^{-3} Torr, and the strongest drying method of 24 h oven-drying at 105 °C, outgas level 6×10^{-3} Torr. There also exists a maximum specific surface area measured for the F-dried sample, outgassed to 6×10^{-3} Torr, namely around 60 m^2/g, again for these experimental conditions and for the drying methods applied. The real specific surface area for the C–S–H gel of the samples prepared under these conditions (w/c ratio, conditions and degree of hydration) should be expected to be above the value obtained by F-drying C^{-t} method. Better microstructure preserving methods, i.e. supercritical drying, should be investigated in the future for this purpose, and also more work to distinguish quantitatively as much as possible between the structural and non-structural water would give more insight into the absence of microporosity for the vacuum-treated samples, and, as a consequence, better understanding of

the effectiveness of the methods and of microstructural implications due to the water removal.

Acknowledgment

The authors wish to thank Dr. J. Rottstegge from the Max-Plank Institute (MPI) for his contribution to this work.

References

[1] Sidney Diamond, Very high strength cement-based materials—a prospective, in: J. Francis Young (Ed.), Materials Research Society, Symposia Proceedings, vol. 42, 1985, pp. 233–243 Pittsburgh, PA.
[2] Jeffry J. Thomas, Hamlin M. Jennings, Andrew J. Allen, The surface area of hardened cement paste as measured by various techniques, Concrete Science and Engineering 1 (1999 March) 45–64.
[3] Ravindra Deshpande, Duen-Wu Hua, Douglas M. Smith, C. Jeffrey Brinker, Pore structure evolution in silica gel during aging/drying. Effects of surface tension, Journal of Non-Crystalline Solids 144 (1992) 32–44.
[4] S. Brunauer, Tobermorite gel: the heart of concrete, American Scientist 50 (1962) 211–229.
[5] S. Brunauer, L. Odler, M. Yudenfreund, The new model of hardened Portland cement paste, Highway Research Record 328 (1970) 89–107.
[6] R.F. Feldman, P. Sereda, A new model for hydrated Portland cement and its practical implications, Engineering Journal of Canada 53 (8–9) (1970) 53–59.
[7] R.F. Feldman, Sorption and length change scanning isotherms of methanol and water on hydrated Portland cement, in: Proc. Fifth Inter. Symp, Chem. Cement, Tokyo, Part III, vol. III-23, 1968, pp. 53–66.
[8] R.A. Helmuth, Dimensional changes and water adsorption of hydrated Portland cement and tricalcium silicate, MSc thesis, Chicago Inst. of Technology, 1965, pp. 58.
[9] G. Litwan, Adsorption isotherm and surface area determination below the triple point, Journal of Physical Chemistry 76 (18) (1972) 2584–2585.
[10] G. Litwan, R.E. Myers, Surface area of cement paste conditioned at various relative humidities. Communicated by F.H. Wittmann, Cement and Concrete Research 13 (1983) 49–60.
[11] F.H. Wittman, Cement production and use. pp. 143–161. Publication No. 79-08, Engineering Foundation, New York.
[12] H.M. Jennings, P.D. Tennis, Model for the developing microstructure in Portland cement pastes. Journal of the American Ceramic Society 77, (12), (1994), 3161–3172 and correction 78, (9) (1995), 2575.
[13] R.F. Feldman, Assessment of experimental evidence for models of hydrated Portland cement, National Research Council. Highway research board, Washington, DC, Highway Research Record 370 (1971) 8–24.
[14] R.F. Feldman, The flow of helium into the interlayer spaces of hydrated Portland cement paste, Cement and Concrete Research 1 (1971) 285–300.
[15] V.S. Ramachandran., R.F. Feldman., J.J. Beaudoin, Concrete Science. Treatise on current research, Heyden & Son, London 1981, pp. 21–22, 55–60, 70–73.
[16] S. Kenneth, W. Sing, Adsorption methods for characterisation of porous materials, Advances in Colloid and Interface Science 76–77 (1998) 3–11.
[17] M.C. Garci Juenger, Hamlin M. Jennings, The use of nitrogen adsorption to access the microstructure of cement paste, Cement and Concrete Research 31 (2001) 883–892.
[18] Maria C. Garci Juenger, Hamlin M. Jennings, Examining the relationship between the microstructure of calcium silicate hydrate and drying shrinkage of cement pastes, Cement and Concrete Research 32 (2002) 289–296.
[19] Jeffry J. Thomas, John H. Seieh, Hamlin M. Jennings, Effect of carbonation on the nitrogen BET surface area of hardened Portland cement paste, Advanced Cement Based Materials 3 (1996) 76–80.
[20] L.E. Copeland, J.C. Hayes, Determination of non-evaporable water in hardened Portland cement paste, ASTM Bulletin (1953 (December)) 70–74.
[21] H.F.W. Taylor, Cement Chemistry, second ed., Telford, London, 1997.
[22] L. Zhang, F.P. Glasser, Critical examination of drying damage to cement pastes, Advances in Cement Research 12 (2) (2000 (Apr.)) 79–88.
[23] L.E., Copel, R.H., Bragg, The hydrates of magnesium perchlorate, Portland Cement Association, Research and development Division, Chicago 10, IL. 1954 1075–1077.
[24] M. Moukwa, P.-C. Aitcin, The effect of drying on cement pastes pore structure as determined by mercury porosimetry, Cement and Concrete Research 18 (1988) 745–752.
[25] C. Galle, Effect of drying on cement-based materials pore structure as identified by mercury intrusion porosimetry. A comparative study between oven-, vacuum-, and freeze-drying, Cement and Concrete Research 31 (2001) 1467–1477.
[26] J.J. Beaudoin, A discussion on, "The use of nitrogen adsorption to access the microstructure of cement paste", in: M.C.G. Juenger, H.M. Jennings (Eds.), Cement and Concrete Research, 32, 2002, pp. 831–832.
[27] H.F.W. Taylor, A.B. Turner, Reactions of tricalcium silicate paste with organic liquids, Cement and Concrete Research 17 (1987) 613.
[28] F.G.R. Gimblett, K.S.W. Sing, Z. Mohd Amin (Grande-Bretagne), Influence of pre-treatment on the microstructure of calcium silicate hydrate gels. 7th International Congress on the Chemistry of Cement, vol. II, Communications, Paris, 1980, pp. 225–231.
[29] F. Roquerol, J. Roquerol, K. Sing, Adsorption by powders and porous solids, Principles, Methodology and Applications, Academic Press, London, 1999.
[30] S. Brunauer, Pore structure of solids, Pure and Applied Chemistry 48 (1976) 401–405.
[31] B.C. Lippens, J.H. DeBoer, Pore-size distribution curves in aluminium oxides system, Journal of Catalysis 3 (1) (1964) 44–49.
[32] C.D. Lawrence, F.G.R. Gimblett, K.S.W. Sing, Sorption of N_2 and n-C_4H_{10} on hydrated cements, in: 7th International Congress on the Chemistry of Cement, vol. III, Communications (Suite), Paris, 1980, pp. 146–151.
[33] S.J. Gregg, K.S.W. Sing, Adsorption, Surface Area and Porosity, 2nd edn. Academic Press, London, 1982.
[34] J.H. De Boer, B.G. Linsen, Th. Van der Plass, H.J. Zondervan, Pore systems in catalysts: VII. Description of the pore dimensions of carbon blacks by the t-method, Journal of Catalysis 4 (1965) 649–653.
[35] Jan Skalny, Ivan Odler, Pore structure of calcium silicate hydrates, Cement and Concrete Research 2 (1972) 387–400.
[36] Sidney Diamond, A discussion of the paper "Effect of drying on cement-based materials pore structure as identified by mercury porosimetry—a comparative study between oven-, vacuum-, and freeze-drying" by C. Gallé, Cement and Concrete Research 33 (2003) 169–170.
[37] R.F. Feldman, Mechanism of creep of hydrated Portland cement paste. Communicated by F.H.Wittmann, Cement and Concrete Research 2 (1972) 521–540.